

# A Digital Implementation of the Nucleus Laminaris

Enrico Heinrich and Ralf Joost and Ralf Salomon

Faculty of Computer Science and Electrical Engineering

University of Rostock

18051 Rostock, Germany

e-mail: {enrico.heinrich,ralf.joost,ralf.salomon}@uni-rostock.de

**Abstract**—The nucleus laminaris of the barn owl auditory system is quite impressive, since its underlying time estimation is much better than the processing speed of the involved neurons. Since precise localization is also very important in many technical applications, this paper explores to what extent the main principles of the nucleus laminaris can be implemented in digital hardware. The first prototypical implementation yields a time resolution of about 20 ps, even though the chosen standard, low-cost device is clocked at only 85 MHz, which leads to an internal duty cycle of approximately 12 ns.

## I. INTRODUCTION

The barn owl auditory system constitutes an impressive localization system [1]. Its performance is mainly due to the architecture of the nucleus laminaris (see, also, Fig. 1). It employs a rather large number of neurons, which all operate as coincidence detectors. These coincidence detectors connect to two reciprocal (anti-parallel) axonal “delay”-lines. These axonal delay lines induce additional delays on the acoustic signals as they travel from one coincidence detector to the next one. In so doing, the axonal delay lines change the mutual timing between the two signals that are originating at the two ears; actually, the timing between the two signals is unique at every coincidence detector. As a consequence all coincidence detectors evaluate a different timing (of the external sound signal), and their spatial distribution corresponds to the location of the external sound signal.

Localization is not only relevant in nature but also in numerous technical applications. The global positioning system

(GPS) [2] (and in the near future, Galileo [3] as well) is one of those examples that have penetrated our everyday life. Despite its wide acceptance, GPS also has a few shortcomings. For example, GPS is not available underneath trees nor is it available in indoor environments, such as buildings and tunnels. Furthermore, GPS yields a precision of roughly 8 m, which can be improved to less than 1 m under certain circumstances.

Due to technological advances, many applications, such as Multimodal Smart Appliance Ensembles for Mobile Applications [4], require robust indoor localization systems, that yield a precision in the range of a 1 cm or below at costs as low as possible. Ubisense [5] and iLoc [6] are very good examples for state-of-the-art indoor localization systems. A further challenge is induced, if electromagnetic signals are to be used, which is often the case; because electromagnetic signals travel with the speed of light  $c = 3 \cdot 10^8$  m/s, a resolution of 1 cm corresponds to approximately 30 ps, which cannot be achieved with currently available low-cost digital systems. Because of these requirements, this paper investigates to which extent the main principles of the nucleus laminaris can be realized in digital hardware. To this end, Section II summarizes the localization problem from a technical point of view.

Section III approaches the *digital implementation* of the neuronal coincidence detectors. Basically, the digital coincidence detector consists of a simple exclusive-or gate, which “mixes” the two incoming signals, and an additional counter, which evaluates gate’s activation time, which directly corresponds to the signals’ difference, i.e., phase shift. Because of its internal structure, this localization system is called exclusively-ored counter array, or X-ORCA for short.

X-ORCA’s internal structure is simple and quite regular. These properties make X-ORCA particularly suitable for the implementation on field-programmable gate arrays (FPGAs) [7] and application-specific integrated circuits (ASICs). An FPGA is a digital circuit that consists of thousands of logical gates, which all can be freely configured as well as freely interconnected at the programmers dispense. Section IV briefly discusses a first prototypical implementation on such a digital device.

The first prototype has been tested in various configurations. Section V summarizes the experimental results, which indicate that the prototype is able to achieve a resolution as small as 20 ps even though the chosen digital device is clocked as slow as 85 MHz, which corresponds to a duty cycle of about

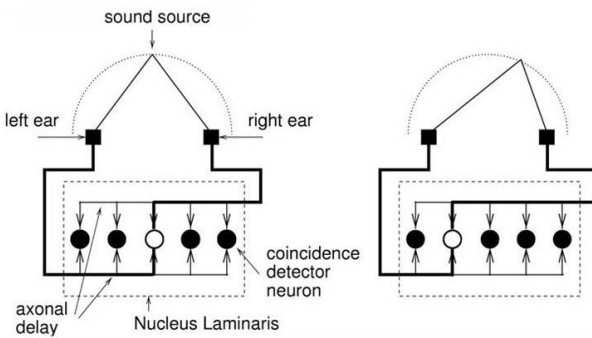


Fig. 1. The barn owl auditory system (nucleus laminaris) consists of a decent number of neurons, which all operate as coincidence detectors and which are all connected to axonal delay lines. Depending on the location of the sound source, all the neurons exhibit different activities.

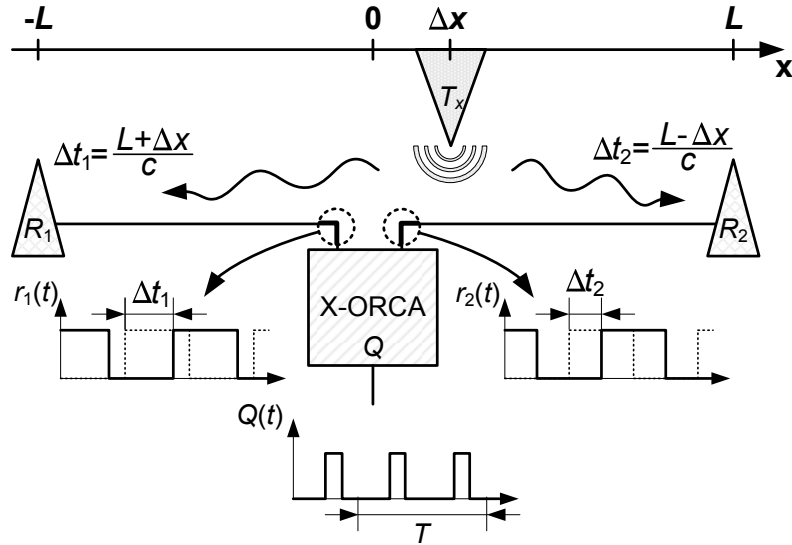


Fig. 2. This paper assumes a standard setup, which is simplified to one dimension here. The two receivers read the transmitter's signals after they have traveled the two distances  $L + \Delta x$  and  $L - \Delta x$ . Thus, the time difference  $\Delta t = t_1 - t_2 = 2\Delta x/c$  is a result of the transmitter's off-center position  $\Delta x$ . The system indirectly determines  $\Delta t = \Delta\varphi/(2\pi f)$  by estimating the phase shift  $\Delta\varphi$  between the two incoming signals  $r_1(t)$  and  $r_2(t)$ .

12 ns. Finally, Section VI concludes this paper with a brief discussion.

## II. PROBLEM DESCRIPTION: LOCALIZATION

Localization is a process that derives new, so-far unknown points from a set of given reference points by evaluating angles and/or distances. Generally, such localization systems come in two flavors: (1) a set of receivers (passive infrastructure) determines the location of an active sender, or (2) a passive receiver derives its own position from the signals emitted by a set of active transmitters. In accordance with the barn owl (and almost all other animals), this paper assumes the first setup.

For educational purpose and for the ease of development, this paper assumes a one-dimensional setup as is illustrated in Figure 2; an extension to a two or three-dimensional setup can be simply realized by duplicating or tripling the one-dimensional setup, and is thus not further discussed in this paper.

In a one-dimensional setup, an active transmitter  $T$  emits a (sound or electromagnetic) signal  $s(t) = A \sin(2\pi f(t - t_0))$  with frequency  $f$ , amplitude  $A$ , and time offset  $t_0$ . After traveling the two distances  $L + \Delta x$  and  $L - \Delta x$ , the signals arrive at the two receivers  $R_1$  and  $R_2$ . Since this traveling happens with a finite speed  $c$ , it arrives at the receivers after the time delays  $\Delta t_1 = (L + \Delta x)/c$  and  $\Delta t_2 = (L - \Delta x)/c$ .

Normally, both receivers employ an amplifier and a Schmitt trigger, which converts any input signal into a rectangular one. Therefore the two receivers provide the rectangular signals  $r_1(t - t_0 - \Delta t_1)$  and  $r_2(t - t_0 - \Delta t_2)$ , with  $\Delta t_1$  and  $\Delta t_2$  denoting the aforementioned time delays that are due to the finite signal traveling speed.

Finally, the localization system has to determine the time difference  $\Delta t = \Delta t_1 - \Delta t_2$  between the two received signals  $r_1(t - t_0 - \Delta t_1)$  and  $r_2(t - t_0 - \Delta t_2)$ . If the localization

system knows the signal frequency  $f$ , it can accomplish this in an indirect way  $\Delta t = \Delta\varphi/(2\pi f)$  by determining the phase shift  $\Delta\varphi$  between the two signals.

It might be, though, that both the physical setup and the localization system have further internal delays, such as switches, cables of different lengths, repeaters, and further logical gates. However, these internal delays can all be omitted, since they can be easily eliminated in a proper calibration process.

Localization by measuring the time-difference-of-arrival becomes particularly challenging, if the system is based on electromagnetic signals, which travel with the speed of light  $c \approx 3 \cdot 10^8$  m/s. For example, an electromagnetic signals travels 1 cm in approximately 33 ps.

## III. THE X-ORCA LOCALIZATION SYSTEM

This section proposes a localization system called X-ORCA, which is an acronym for XOR-ed counter array. On an abstract level, this system has quite the same architecture as the barn owl auditory systems. It consists of two inputs (the two ears), two regular wires (the two axonal delays), and quite a number of coincidence detectors (the neurons).

The description of the (digital) coincidence detectors requires a little more care. First of all, simple logic gates cannot be operating as coincidence detectors. Then, “coincidence” of two signals can be interpreted such that there is no difference between them; in other words, they are identical at all times. The difference of two signals is easy to detect, a simple XOR gate does the job. An XOR gate delivers a logical one, if either of the two inputs has a logical one but not both. Thus, the proportion of a logical one with respect to a logical zero at the output of an XOR gate expresses the phase shift  $\varphi$  between the two inputs (see, also, Section II).

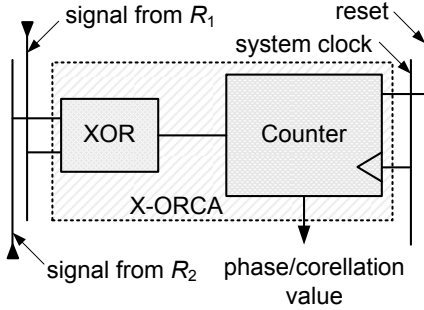


Fig. 3. The combination of a simple XOR gate and a subsequent counter is able to operate as a coincidence detector. The counter value is proportional to the proportion of logical ones at the XOR gate's output and the total number of clock cycles. The counter value is thus proportional to the phase shift  $\Delta\varphi$  between both input signals.

With an XOR gate as the combiner of the two inputs, the task is to measure the average duration of the logical ones at its output. This can be achieved with the circuitry illustrated in Figure 3. The output of the XOR gate is connected to the enable input of a simple counter. This counter increases its value, if at the clock signal (actually the transition from a logical zero to a logical one), the enable input is activated. Thus, the counter value is proportional to the timely proportion of logical ones at the XOR gate's output and the total number of clock cycles. This value is thus proportional to the phase shift  $\Delta\varphi$  between both input signals.

For example, let us assume an input signal with a frequency of  $f = 100 \text{ MHz}$  and a phase shift of  $\Delta\varphi = \pi/4 = 45^\circ$ . Then, if the counter is clocked at a rate of  $10 \text{ GHz}$  over a signal's period  $T = 1/(100 \text{ MHz}) = 10 \text{ ns}$ , the counter will assume a value of  $v = 25$ . In this example, all the given numbers, particularly the chosen frequencies, are for educational purposes only, and may not be realistic in a specific implementation.

As has already been seen in the barn owl auditory system, X-ORCA also employs a large number of coincidence detectors (see Figure 3), which are all connected to two reciprocal (anti-parallel) “delay” wires  $w_1$  and  $w_2$  on which the two signals  $r_1(t)$  and  $r_2(t)$  travel with approximately two third of the speed of light  $c_w \approx 2/3c$ .

The mode of operation of the X-ORCA system is quite identical to that of the barn owl. Let us start with the coincidence detector (neurons) at which the two inputs match, i.e., both inputs have a vanishing phase shift  $\varphi = 0$ . Then, due to the “delays” along the two wires  $w_1$  and  $w_2$ , the coincidence detectors to the right and left observe non-matching inputs, i.e., non-vanishing phase shifts  $\varphi \neq 0$ . If the delay wires cause a time delay  $\delta$  between two coincidence detectors, then these detectors observe a total time shift of  $2\delta$ . That is, the duration of a logical one is also increased or decreased by  $2\delta$ .

Normally, the time difference  $2\delta$  is much smaller than the duty cycle of the counter, and would thus not have any effect. However, if sampling over a sufficiently long time span, this tiny time delay will eventually affect the final counter value.

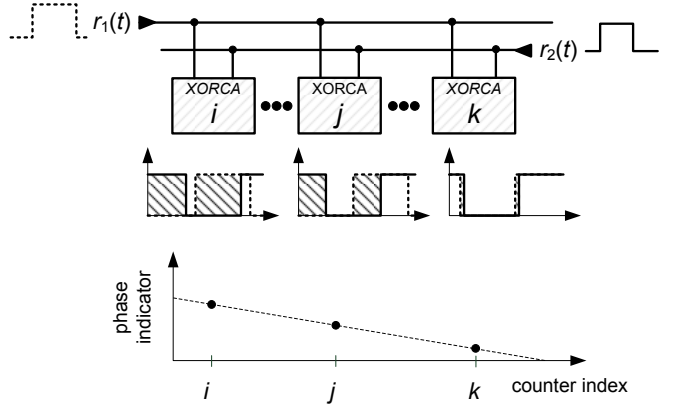


Fig. 4. X-ORCA places all phase detectors along two reciprocal (anti-parallel) “delay” wires  $w_1$  and  $w_2$  on which the two signals  $r_1(t)$  and  $r_2(t)$  travel with approximately two third of the speed of light  $c_w \approx 2/3c$ . Because the two wires  $w_1$  and  $w_2$  are reciprocal, all phase detectors have different internal delays  $\tau_i$ .

#### IV. THE FIRST PROTOTYPE

The first X-ORCA prototype was implemented on an Altera Cyclone II FPGA [8]. This device charges about 50 USD, offers 33,216 logic elements, and can be clocked at about 85 MHz. The *development board*, which is required only during research and development, charges about 500 USD and features all the required components, interfaces, and development tools.

On the top-level view, the X-ORCA prototype consists of 140 phase detectors, a common data bus, a Nios II soft core processor [9], and a system PLL that runs at 85 MHz. The Nios II processor manages all the counters of the phase detectors, and reports the results via an interface to a PC.

Due to the limited laboratory equipment, the transmitter is realized as a simple function generator that emits a sinusoidal signal. In order to focus on the core system, wireless communication capabilities were not employed; rather, the prototype is connected to the function generator via a regular wire as well as a line stretcher [10]. Such a line stretcher can be extended or shorted, and can thus change the signal propagation time accordingly.

It should be noted, though, that X-ORCA's internal “delay wires”  $w_1$  and  $w_2$  are realized as pure passive internal wires, connecting the device's logic elements, as previously announced in Section III.

#### V. RESULTS

Figures 5-10 summarize the experimental results that were achieved by the first X-ORCA prototype under different configurations. Unless otherwise stated, these figures present the counter values  $v_i$  of  $n = 140$  different phase detectors, which were clocked at a rate of 85 MHz.

Figure 5 shows the behavior of the X-ORCA architecture when using the external 19 MHz localization signal. In this experiment, one of the connections from the function generator to the input pad of the development board was established

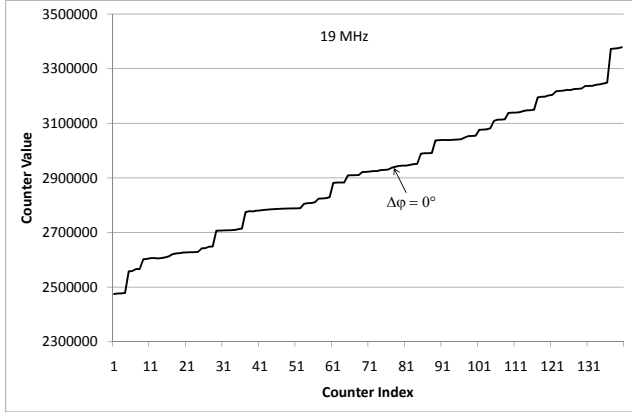


Fig. 5. The figure shows the counter values  $v_i$  of  $n = 140$  phase detectors when fed with two 19 MHz signals with zero phase shift  $\Delta\varphi = 0$ .

by a line stretcher [10], whereas the other one was made of a regular copper wire. Figure 5 shows the values  $v_i$  of the  $n = 140$  counters, which were still clocked at 85 MHz over a measurement period of 10,000,000 ticks.

In addition, Figure 5 reveals some technological FPGA internals that might be already known to the expert reader: neighboring logic elements do not necessarily have equivalent technical characteristics and are not interconnected by a regular wire grid. As a consequence, the counter values  $v_i$  and  $v_{i+1}$  of two neighboring phase detectors do not steadily increase or decrease, which makes the curve look a bit rough. This effect can be compensated. Each counter has a unique and constant internal delay, therefore, the counter values  $v_i$  can be plotted over the internal delay  $\tau_i$  that results in a flat curve as shown in Figure 6.

The three graphs in Figure 6 refer to a phase shift of  $\Delta\varphi \in \{-0.3^\circ, 0, +0.3^\circ\}$ , which corresponds to time delays  $\Delta t \in -0.02 \text{ ns}, 0 \text{ ns}, +0.02 \text{ ns}$ . It should be noted that the graph of

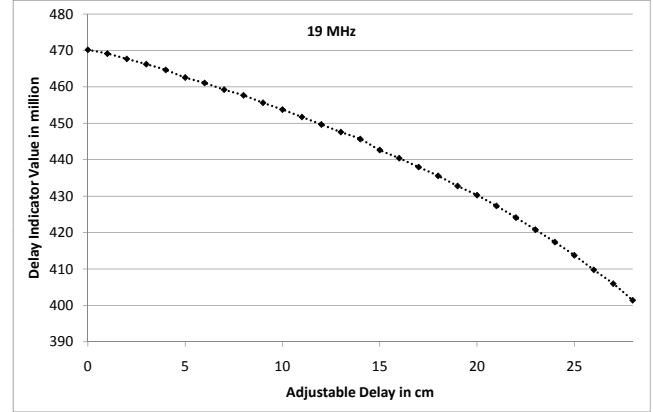


Fig. 7. The figure shows the delay value indicator resulting from adjustable delay line lengths when fed with two 19 MHz signals.

this figure appears as a straight line, since the internal time delays  $\tau_i$  span much less than an entire period of the 19 MHz signal.

Figure 7 presents a different view of Figure 6: In the graph, every dot represents the sum  $v_{\text{tot}} = \sum_i v_i$  of all  $n = 140$  counter values  $v_i$ ; that is, an entire graph of Figure 6 is collapsed into one single dot. The graph shows 29 measurements in which the line stretcher was extended by 1 cm step by step. It can be seen that a length difference of  $\Delta x = 1 \text{ cm}$  decreases  $v_{\text{tot}}$  by about 20 million. This result suggests that with a localization of 19 MHz, X-ORCA is able to detect a length difference of about  $\Delta x = 1 \text{ mm}$ , which equals a time resolution of about 0.02 ns.

The second focus of the practical experiments was to explore the lower limit of the normalized time delay  $\Delta t/f$ . To this end, the prototype was exposed to two localization signals with varying time delays. The localization frequencies were set to  $f \in \{1.14 \text{ MHz}, 111 \text{ kHz}, 11 \text{ kHz}\}$ . The results are plotted in Figures 8-10.

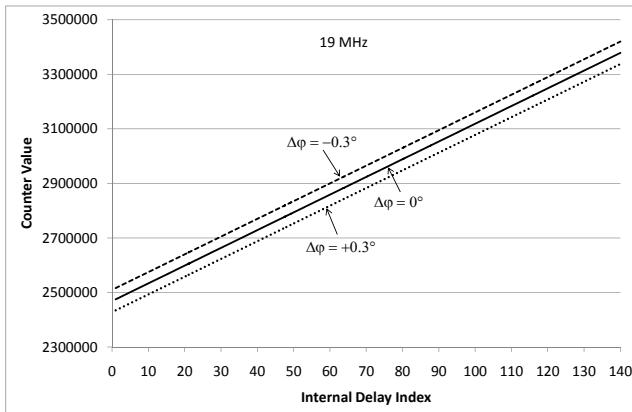


Fig. 6. The figure shows the derived counter values  $v_i$  of  $n = 140$  phase detectors when fed with two 19 MHz signals with zero phase shift  $\Delta\varphi = 0$  (dashed line), with about  $-0.3^\circ$  phase shift  $\Delta\varphi \approx -0.3^\circ$  (solid line), and with about  $+0.3^\circ$  phase shift  $\Delta\varphi \approx +0.3^\circ$  (dash-dot line).

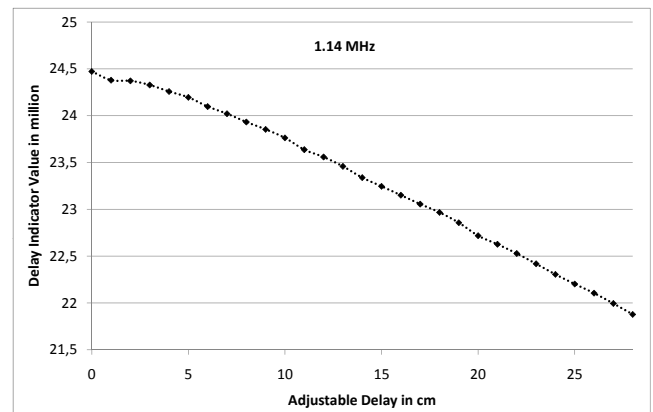


Fig. 8. The figure shows the delay value indicator when employing two 1.14 MHz localization signals. The data points results from varying length of the employed line stretcher.

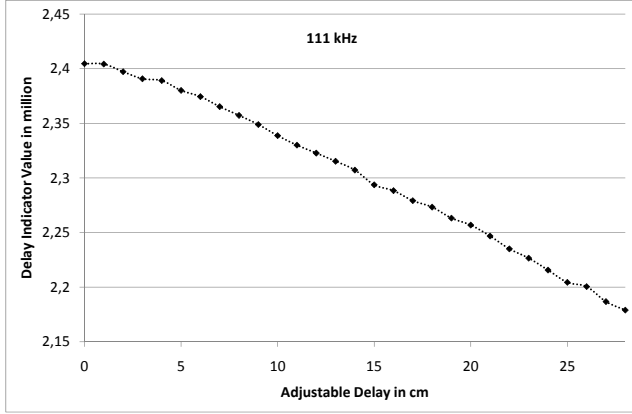


Fig. 9. The figure shows the delay value indicator when employing two 111 kHz localization signals. The data points results from varying length of the employed line stretcher.

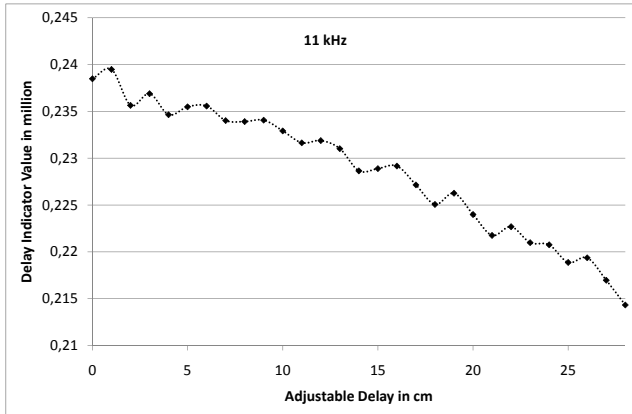


Fig. 10. The figure shows the delay value indicator when employing two 11 kHz localization signals. The data points results from varying length of the employed line stretcher.

All three figures show the very same qualitative behavior. The only difference is the absolute value of the delay value indicator: a decrease of the localization frequency by a factor of 10 leads to a reduction of the delay value indicator by the very same amount; with the identical time delay  $\Delta t$  the phase shift is only a tenth, if the frequency is also just a tenth.

## VI. DISCUSSION

This paper has argued that it is always required to utilize (artificial) evolutionary algorithms in order to solve open technical problems. For some problems, nature has already evolved optimal solutions. In that case, the natural solution has to be transferred to the technical application at hand.

As an example, this paper has analyzed the barn owl auditory system, since its resolution is much better than the processing speed of the neurons would allow. The barn owl achieves its impressive resolution by (1) employing a large number of coincidence detectors, which are (2) all connected to two passive axonal delay lines.

This paper has proposed a digital implementation of the core concepts of the nucleus laminaris as can be found in the barn owl auditory system. Due to its internal structure, this architecture is called X-ORCA, and has been prototypically implemented on a standard, low-cost FPGA. This prototype yields a time resolution of about 20 ps, which is about three orders of magnitude better than the duty cycle of the digital device.

During 20 ps, an electromagnetic signal travels roughly 6 mm. With this performance, X-ORCA might be used as the core of a complete localization system, even in its current, rather preliminary state.

Future research will be devoted to the following avenues. First, the system's limits will be explored by utilizing improved laboratory equipment. And Second, future research will also be devoted to the integration of wireless communication modules. The best option for that approach seems to be the utilization of a software-defined radio module, such as the Universal Software Radio Peripheral 2 (USRP2) [11]. Finally, future research will port the first prototype onto more state-of-the-art development boards, such as an Altera Stratix V FPGA [12].

## ACKNOWLEDGEMENTS

The authors gratefully thank Volker Kühn and Sebastian Vorköper for their helpful discussions. This work was supported in part by the DFG graduate school 1424. Special thanks are due to Matthias Hinkfot for valuable comments on draft versions of the paper.

## REFERENCES

- [1] R. Kempter, W. Gerstner, and J. L. van Hemmen, "Temporal coding in the sub-millisecond range: Model of barn owl auditory pathway," *Advances in Neural Information Processing Systems*, vol. 8, pp. 124–130, 1996.
- [2] P. Misra and P. Enge, "Global positioning system: Signals, measurements, and performance," in *2nd Edition, Ganya-Jamuna Press*, 2006.
- [3] *The Galileo Project - GALILEO Design consolidation*, European Commission, 2003.
- [4] Multimodal Smart Appliance Ensembles for Mobile Applications (MuSAMA) project page, <http://www.informatik.uni-rostock.de/musama.html>.
- [5] Ubisense Ltd., <http://www.ubisense.net>.
- [6] S. Knauth, C. Jost, and A. Klapproth, "iloc: a localisation system for visitor tracking & guidance," in *Proceedings of the 7th IEEE International Conference on Industrial Informatics 2009 (INDIN 2009)*, 2009, pp. 262–266.
- [7] *Cyclone II Device Handbook*, Altera Corp., San Jose, CA, 2007, Altera Document CII51002-3.1.
- [8] *Nios Development Board Cyclone II Edition Reference Manual*, Altera Corp., San Jose, CA, 2007, altera Document MNLN051805-1.3.
- [9] *Nios II Processor Reference Handbook*, Altera Corp., San Jose, CA, 2007, Altera Document NIISV1-7.2.
- [10] *Microlab: "Line Stretchers, SR series"*, Datasheet, Microlab Company, 2008.
- [11] Ettus Research LLC, <http://www.ettus.com>.
- [12] *Stratix V Device Handbook*, Altera Corp., San Jose, CA, 2010, Altera Document SV5V1-1.0.